NIKHEF/2000-005
hep-ph/0003318

Helicity Amplitudes for Single-Top Production

J. van der Heide, E. Laenen, L. Phaf and S. Weinzierl

NIKHEF Theory Group
Kruislaan 409, 1098 SJ Amsterdam, The Netherlands

arXiv:hep-ph/0003318v2 2 Oct 2000

Abstract

Single top quark production at hadron colliders allows a direct measurement of the top quark charged current coupling. We present the complete tree-level helicity amplitudes for four processes involving the production and semileptonic decay of a single top quark: W-gluon fusion, flavor excitation, s-channel production and W-associated production. For the first three processes we study the quality of the narrow top width approximation. We also examine momentum and angular distributions of some of the final state particles.

1 Introduction

Of the properties of the top quark, discovered at the Fermilab Tevatron [1, 2], so far only its mass has been directly measured, and, to some extent, its QCD coupling strength via the total production cross section. There is hope to measure its charged-current coupling, both in strength and handedness, via single-top production at hadron colliders [3] - [19] in Run II at the Tevatron.

Besides having obvious intrinsic value, this measurement has additional importance because the charged-current top coupling might be particularly sensitive to certain signals of new physics [9], [15], [20] - [29]. Our context here is however the Standard Model.

To be sure, isolating a clear signal for single top production will not be easy, in view of the complicated final state and the many backgrounds, such as $t\bar{t}$ production. Valuable work has recently been done on constructing optimal signal definitions, and examining corresponding backgrounds and acceptances [16, 17, 30].

There are various partonic subprocesses that lead to the production of a single top. The ones for which we derive tree-level helicity amplitudes are the "W-gluon fusion" process

$$u + g \to t + d + \bar{b}, \tag{1}$$

the "flavor excitation" process

$$u + b \to t + d, \tag{2}$$

the Drell-Yan like "s-channel" process, which occurs via a virtual timelike W-boson

$$u + \bar{d} \to t + \bar{b}, \tag{3}$$

and the "W-associated" production process

$$g + b \to t + W \tag{4}$$

with the W decaying hadronically. In reactions (1) and (2) it is understood that we may replace the (u, d)-quark pair by $(\bar{d}, \bar{u})$, (c, s) and $(\bar{s}, \bar{c})$. In reaction (3) we may replace the $(u, \bar{d})$-pair by $(c, \bar{s})$. In addition, CKM suppressed combinations may be included.

Because of its large mass, the electroweak decay of the top quark proceeds so rapidly that top bound states do not have time to form [31]. This also means that the decay products of the top quark are correlated with its spin. It is therefore desirable to include the semileptonic decay[1] of the top quark in the amplitudes:

$$t \to b + \bar{l} + \nu. \tag{5}$$

The complete tree-level amplitudes for flavor-excitation and s-channel production can be obtained by crossing from those for

$$0 \to b + \bar{l} + \nu + \bar{b} + \bar{u} + d. \tag{6}$$

[1]Single-top production with hadronic top decay suffers from large QCD backgrounds.

with "0" representing the vacuum. Likewise, the amplitudes for W-gluon fusion and W-associated production are obtained by crossing from

$$0 \to b + \bar{l} + \nu + \bar{b} + \bar{u} + d + g \tag{7}$$

In this paper we present the complete tree-level helicity amplitudes for (6) and (7). We obtain compact expressions by using spinor helicity methods. We present in addition all amplitudes for the subprocesses (1-4) in the narrow top width approximation [32, 33]. This allows us to check the quality of this approximation against the full calculation, for which only a few of the diagrams actually involve a top quark.

Although the helicity amplitudes for (1-4), including top decay, may be obtained as well as Fortran code from the program Madgraph [34], we believe that our analytical results are valuable for a number of reasons. First, analytical expressions can offer additional insights, e.g. in the phase space structure of the cross section near the top mass pole. Second, they lead to even more compact computer codes by allowing numerical crossing, and third, they allow evaluation in terms of spinor products, and in different computer languages (we use C++). Finally, our results constitute a nontrivial check on this useful program. In this context we also mention the program Onetop [35], and the general purpose programs Pythia [36] and Herwig [37] which can be used as event generators for single top production.

In order to test these amplitudes numerically, we study various distributions in momentum and angle of some of the final state particles for each process separately. We limit ourselves here to the subprocesses (1-3), because process (4) is negligible [12, 16] at the Tevatron. We note that whether a subprocess is a leading order contribution or a higher order correction to another, depends on the definition of the final state. Thus, for sufficiently inclusive quantities the W-gluon fusion and flavor excitation processes are not independent: a part of the former is then in fact a higher order QCD correction to the latter, and must be mass factorized [3]. A similar argument applies to W-gluon fusion and the s-channel process in the case where the gluon couples to the u-d-quark line, and the signal is defined to be inclusive with respect to the presence of the light quark jet. Furthermore, whether bottom quarks are part of the initial state is a choice of factorization scheme. We adopt a five-flavor scheme and include bottom quark parton distribution functions. In this paper we wish to examine some characteristics of each process individually, rather than perform a comprehensive phenomenological study involving combinations of these processes and their backgrounds, as such studies already exists in the literature [16, 17]. We therefore focus on exclusive quantities, e.g. we require exactly three jets or exactly two jets.

Our conventions for spinor helicity methods are listed in section 2. Sections 3 and 4, together with appendices A and B, contain the helicity amplitudes for processes (6) and (7). In section 5 we discuss the narrow top width approximation, while the results of our numerical studies can be found in section 6. We conclude in section 7.

2 Spinor helicity

To compute the amplitudes for (6) and (7) we use spinor helicity methods [38] - [42]. We limit ourselves here to listing our conventions, for reviews of spinor helicity methods see e.g. [43, 44].

With spinor helicity methods we can express scattering amplitudes in terms of massless Weyl spinors of helicity $\pm\frac{1}{2}$

$$u(p,\pm) = v(p,\mp) = |p\pm\rangle\,, \qquad \bar{u}(p,\pm) = \bar{v}(p,\mp) = \langle p\pm|\,. \tag{8}$$

External fermion states are directly expressed in terms of these. Our convention is to take all particles outgoing. For example an outgoing massless fermion with positive helicity is denoted by $\langle p+|$, while an outgoing massless antifermion with positive helicity is denoted by $|p-\rangle$. The gluon polarization vectors, of helicity ±1, may be written as

$$\varepsilon^+_\mu(k,q) = \frac{\langle q-|\gamma_\mu|k-\rangle}{\sqrt{2}\langle qk\rangle}, \qquad \varepsilon^-_\mu(k,q) = \frac{\langle q+|\gamma_\mu|k+\rangle}{\sqrt{2}[kq]}. \tag{9}$$

We have used the customary short-hand notation:

$$\langle ij\rangle = \langle p_i - |p_j+\rangle, \qquad [ij] = \langle p_i + |p_j-\rangle. \tag{10}$$

In (9) k is the gluon momentum and q an arbitrary light-like "reference momentum". The dependence on the choice of q drops out in gauge-invariant amplitudes. We shall also employ the abbreviations

$$\begin{aligned} \langle i-|k+l|j-\rangle &= \langle ik\rangle[kj] + \langle il\rangle[lj], \\ s_{ij\ldots k} &= (p_i + p_j + \ldots + p_k)^2\,, \end{aligned} \tag{11}$$

with all momenta null-vectors.

To investigate the narrow-width approximation (section 5), we must treat the massive top quark as an external state. Appropiately extended spinor techniques exist ([39], [45] - [47]). Even though helicity is not a conserved quantum number for a massive particle, a massive positive-energy spinor satisfying the Dirac equation has a two-fold degeneracy (e.g. labelled by a spin-component quantized along some axis). With slight abuse of notation we label these two states by "+" and "−". Let p be a four-vector with $p^2 = m^2$ and $p_0 > 0$, and let q be an arbitrary null vector with $q_0 > 0$. We define

$$\begin{aligned} u(p,+) &= \frac{1}{\sqrt{2pq}}\,(\not{p}+m)\,|q-\rangle, \qquad v(p,+) = \frac{1}{\sqrt{2pq}}\,(\not{p}-m)\,|q-\rangle, \\ u(p,-) &= \frac{1}{\sqrt{2pq}}\,(\not{p}+m)\,|q+\rangle, \qquad v(p,-) = \frac{1}{\sqrt{2pq}}\,(\not{p}-m)\,|q+\rangle. \end{aligned} \tag{12}$$

For the conjugate spinors we have

$$\begin{aligned} \bar{u}(p,+) &= \frac{1}{\sqrt{2pq}}\langle q-|\,(\not{p}+m)\,, \qquad \bar{v}(p,+) = \frac{1}{\sqrt{2pq}}\langle q-|\,(\not{p}-m)\,, \\ \bar{u}(p,-) &= \frac{1}{\sqrt{2pq}}\langle q+|\,(\not{p}+m)\,, \qquad \bar{v}(p,-) = \frac{1}{\sqrt{2pq}}\langle q+|\,(\not{p}-m)\,. \end{aligned} \tag{13}$$

It is easy to check that for these spinors the Dirac equations, orthogonality and completeness relations hold. A massive quark propagator may be expressed in terms of massless Weyl spinors via

$$\frac{i\delta_{ij}}{p^2 - m^2 + i\epsilon} \left(p_+ + p_- + m \right), \tag{14}$$

where p_+ and p_- are of the form

$$\begin{aligned} p_+ &= |p_1+\rangle\langle p_1+| \ + ... + \ |p_n+\rangle\langle p_n+| \\ p_- &= |p_1-\rangle\langle p_1-| \ + ... + \ |p_n-\rangle\langle p_n-| \end{aligned} \tag{15}$$

for some nullvectors p_1,...,p_n.

For all other vertices and propagators we use standard Feynman rules, in the conventions of [48], and the 't Hooft-Feynman R_ξ-gauge with $\xi = 1$. We neglected all fermion masses except the top mass. As a consequence, neither diagrams containing a Higgs boson nor diagrams with would-be Goldstone bosons contribute.

3 W-gluon fusion and W-associated production

In this section we present the helicity amplitudes for the process

$$0 \to \nu(p_1) + \bar{l}(p_2) + b(p_3) + \bar{b}(p_4) + g(p_5) + d(p_6) + \bar{u}(p_7). \tag{16}$$

The amplitudes are calculated in tree approximation at order $O(g g_w^4)$, where g denotes the strong coupling and g_w the electroweak coupling. There are also tree diagrams of order $O(g^3 g_w^2)$ ("QCD + Weak") contributing to (16). This gauge-invariant set of graphs does not contain a top quark as an intermediate state, and we do not consider it in this paper.

The results for the (W-gluon fusion) processes $u + g \to \nu + \bar{l} + b + \bar{b} + d$ and $\bar{d} + g \to \nu + \bar{l} + b + \bar{b} + \bar{u}$, as well as for the (W-associated) process $b + g \to \nu + \bar{l} + b + d + \bar{u}$, can be obtained from those of process (16) by crossing, under which the crossed momentum and helicity change sign. The color decomposition for the amplitude (16) reads

$$A_{Wg} = g T^a_{34} \delta_{67} A^{(1)}_{Wg} + g \delta_{34} T^a_{67} A^{(2)}_{Wg}. \tag{17}$$

The partial amplitudes $A^{(1)}_{Wg}$ and $A^{(2)}_{Wg}$ are gauge-invariant by themselves. $A^{(1)}_{Wg}$ corresponds to diagrams where the gluon couples to the b-$\bar{b}$-fermion line, whereas $A^{(2)}_{Wg}$ involves the gluon coupling to the d-$\bar{u}$-fermion line. Representative Feynman diagrams for the partial amplitudes $A^{(1)}_{Wg}$ and $A^{(2)}_{Wg}$ are shown in Fig. 1 and Fig. 2, respectively. There are 21 diagrams contributing to $A^{(1)}_{Wg}$, 3 of them contain a top quark. The partial amplitude $A^{(2)}_{Wg}$ is made up of 24 diagrams, with 2 containing a top quark.

For the color matrices we have used the short-hand notation $T^a_{34} = T^a_{i_3 j_4}$. They are normalized as

$$\mathrm{Tr}\ T^a T^b = \frac{1}{2} \delta^{ab}. \tag{18}$$

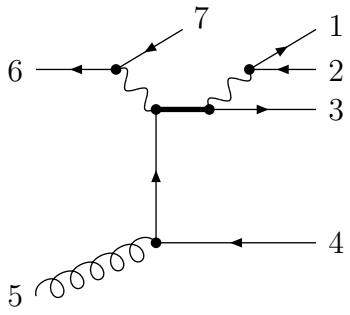

Figure 1: *A representative Feynman diagram for single-top production contributing to the partial amplitude $A^{(1)}_{Wg}$ (17). The top quark line is thickened.*

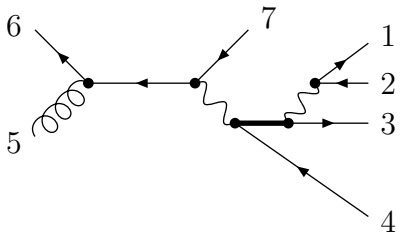

Figure 2: *A representative Feynman diagram for single-top production contributing to the partial amplitude $A^{(2)}_{Wg}$ (17). The top quark line is thickened.*

We can decompose the two subamplitudes in (17) further according to their electroweak structure:

$$\begin{aligned}
A_{Wg}^{(1)} &= \frac{e^4 V_{ud}^*}{2\sin^2\theta_W}\left(\frac{||V_{tb}||^2}{2\sin^2\theta_W}A_{Wg}^{(1,1)} + \left(v_d^\gamma v_b^\gamma + v_d^Z v_b^Z \mathcal{P}_Z(s_{345})\right)A_{Wg}^{(1,2)}\right. \\
&+ \left(v_u^\gamma v_b^\gamma + v_u^Z v_b^Z \mathcal{P}_Z(s_{345})\right)A_{Wg}^{(1,3)} + \left(v_b^\gamma - \frac{\cos\theta_W}{\sin\theta_W}v_b^Z\mathcal{P}_Z(s_{345})\right)A_{Wg}^{(1,4)} \\
&+ \left(v_e^\gamma v_b^\gamma + v_e^Z v_b^Z \mathcal{P}_Z(s_{345})\right)A_{Wg}^{(1,5)} + \left. v_\nu^Z v_b^Z \mathcal{P}_Z(s_{345})A_{Wg}^{(1,6)}\right), \\
A_{Wg}^{(2)} &= \frac{e^4 V_{ud}^*}{2\sin^2\theta_W}\left(\frac{||V_{tb}||^2}{2\sin^2\theta_W}A_{Wg}^{(2,1)} + \left(v_d^\gamma v_b^\gamma + v_d^Z v_b^Z \mathcal{P}_Z(s_{34})\right)A_{Wg}^{(2,2)}\right. \\
&+ \left(v_u^\gamma v_b^\gamma + v_u^Z v_b^Z \mathcal{P}_Z(s_{34})\right)A_{Wg}^{(2,3)} + \left(v_b^\gamma - \frac{\cos\theta_W}{\sin\theta_W}v_b^Z\mathcal{P}_Z(s_{34})\right)A_{Wg}^{(2,4)} \\
&+ \left(v_e^\gamma v_b^\gamma + v_e^Z v_b^Z \mathcal{P}_Z(s_{34})\right)A_{Wg}^{(2,5)} + \left. v_\nu^Z v_b^Z \mathcal{P}_Z(s_{34})A_{Wg}^{(2,6)}\right).
\end{aligned} \tag{19}$$

Here

$$\begin{aligned}
\mathcal{P}_Z(s) = \frac{s}{s-m_Z^2}, \qquad & e = g_w \sin\theta_W \\
v_f^{\gamma,L} = -Q, \qquad & v_f^{\gamma,R} = -Q \\
v_f^{Z,L} = \frac{I_3 - Q\sin^2\theta_W}{\sin\theta_W\cos\theta_W}, \qquad & v_f^{Z,R} = \frac{-Q\sin\theta_W}{\cos\theta_W},
\end{aligned} \tag{20}$$

where Q and I_3 denote the charge and the third component of the weak isospin of the fermion. The labels L and R denote the left- and right-handed couplings. Further, θ_W denotes the Weinberg angle and V_{ud} and V_{tb} denote CKM-matrix elements.

Because the W-boson only couples to left-handed fermions, all non-vanishing amplitudes have the helicity configuration $(p_1^-, p_2^+, p_6^-, p_7^+)$. Furthermore the helicity along the fermion line $b(p_3)$-$\bar{b}(p_4)$ is conserved. Due to their number and length we have collected the explicit expressions for the partial helicity amplitudes $A_{Wg}^{(k,l)}$ in (19) in appendix A. We have verified the correctness of these expressions by numerical comparison with the computer code generated by Madgraph [34].

The cross section for W-gluon fusion, summed and averaged over helicities and colours is then given by

$$\sigma_{Wg} = \sum_{i,j}\int dx_1 f_i(x_1)\int dx_2 f_j(x_2)\int d\phi_5 \frac{1}{8\hat{s}}\sum_{helicities}\frac{1}{2}\left(\left|A_{Wg}^{(1)}\right|^2 + \left|A_{Wg}^{(2)}\right|^2\right)\Theta(\text{cuts}) \tag{21}$$

where $f_i(x_1)$ and $f_j(x_2)$ are the parton densities of the initial partons i and j, $d\phi_5$ denotes the phase space measure for five massless particles, $2\hat{s}$ is the flux factor, $\Theta(\text{cuts})$ represents the jet-defining cuts and $A_{Wg}^{(1)}$ and $A_{Wg}^{(2)}$ are the amplitudes in (19) with partons i and j crossed into the initial state.

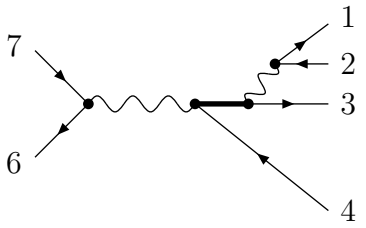

Figure 3: *A representative Feynman diagram corresponding to the partial amplitude $A^{(1)}_{Wb}$ (23). The top quark line is thickened.*

4 Flavor excitation and s-channel

The helicity amplitudes for both these processes can be obtained by crossing from

$$0 \to \nu(p_1) + \bar{l}(p_2) + b(p_3) + \bar{b}(p_4) + d(p_6) + \bar{u}(p_7). \tag{22}$$

The tree-level amplitudes correspond to order $O(g_w^4)$. To this order the color decomposition of the amplitude for (22) is simply

$$A_{Wb} \;=\; \delta_{34}\delta_{67}A^{(1)}_{Wb} \tag{23}$$

since no gluons are involved. A representative Feynman diagram is shown in Fig. 3. There are 10 Feynman diagrams contributing to this amplitude, only one of them contains a top quark. We write the partial amplitudes $A^{(1)}_{Wb}$ as

$$\begin{aligned} A^{(1)}_{Wb} \;=\; & \frac{e^4 V^*_{ud}}{2\sin^2\theta_W}\left(\frac{||V_{tb}||^2}{2\sin^2\theta_W}A^{(1,1)}_{Wb} + \left(v^\gamma_d v^\gamma_b + v^Z_d v^Z_b \mathcal{P}_Z(s_{34})\right) A^{(1,2)}_{Wb}\right. \\ & + \left(v^\gamma_u v^\gamma_b + v^Z_u v^Z_b \mathcal{P}_Z(s_{34})\right) A^{(1,3)}_{Wb} + \left(v^\gamma_b - \frac{\cos\theta_W}{\sin\theta_W} v^Z_b \mathcal{P}_Z(s_{34})\right) A^{(1,4)}_{Wb} \\ & \left. + \left(v^\gamma_e v^\gamma_b + v^Z_e v^Z_b \mathcal{P}_Z(s_{34})\right) A^{(1,5)}_{Wb} + v^Z_\nu v^Z_b \mathcal{P}_Z(s_{34}) A^{(1,6)}_{Wb}\right). \end{aligned} \tag{24}$$

All helicity amlitudes have the helicities (p_1^-, p_2^+) and (p_6^-, p_7^+). Again the helicity along the b-$\bar{b}$-line is conserved. The explicit expressions for the $A^{(1,k)}_{Wb}$ in (24) are collected in appendix B.

We have checked these results numerically with the computer code produced by Madgraph [34], and found agreement. For the present process we could in addition compare to results produced by the Comphep program [49], and found agreement as well. With the helicity amplitudes at hand one obtains the cross section for flavor excitation, summed and averaged over helicities and colors, as

$$\sigma_{Wb} \;=\; \sum_{i,j}\int dx_1 f_i(x_1)\int dx_2 f_j(x_2)\int d\phi_4 \frac{1}{8\hat{s}} \sum_{helicities} \left|A^{(1)}_{Wb}\right|^2 \Theta(\text{cuts}) \tag{25}$$

with $d\phi_4$ the phase space measure for 4 massless particles and i and j label the partons crossed for flavor excitation. The cross section for the s-channel process is obtained in a similar way by crossing the appropriate partons.

There are tree diagrams of order $O(g^2 g_w^2)$ that contribute to (22). As they are a separately gauge-invariant set and do not contain a top quark they are not directly relevant to us here. However, for this case we do present these "QCD + Weak"-amplitudes because they may be easily obtained from the $O(g_w^4)$ tree amplitudes, as follows

$$A_{\rm QCD+Weak} = \frac{1}{2}\left(\delta_{37}\delta_{64} - \frac{1}{N_c}\delta_{34}\delta_{67}\right)\frac{g^2 e^2 V_{ud}^*}{2\sin^2\theta_W}\left(A_{Wb}^{(1,2)} + A_{Wb}^{(1,3)}\right), \tag{26}$$

where N_c denotes the number of colors. In contrast to the process of the previous section, these "QCD + Weak"-amplitudes do not interfere with the $O(g_w^4)$ amplitudes.

5 Narrow width approximation

By including the top quark semileptonic decay in the amplitudes for (6) and (7), we must include as well many diagrams in which no top is present. Therefore it is interesting to know to what extent results are approximated by producing the top quark as an on-shell particle, whose decay happens independently from its production.

A numerical indication that the narrow top width approximation for the W-gluon, s-channel and W-associated processes works well is already present in [16]. Here we examine this issue both numerically and analytically for the three subprocesses (1), (2)[2] and (3). Thus we need the helicity amplitudes for the W-gluon fusion process without top decay

$$0 \to t(p_8) + \bar{b}(p_4) + g(p_5) + d(p_6) + \bar{u}(p_7). \tag{27}$$

The amplitude may again be color-decomposed as

$$A_{Wg,prod} = gT^a_{84}\delta_{67}A^{(1)}_{Wg,prod} + g\delta_{84}T^a_{67}A^{(2)}_{Wg,prod} \tag{28}$$

with

$$\begin{aligned} A^{(1)}_{Wg,prod} &= \frac{e^2 V_{ud}^* V_{tb}}{2\sin^2\theta_W}\cdot\frac{(-i)2\sqrt{2}}{s_{67}-m_W^2}\frac{B^{(1)}_{Wg,prod}}{\sqrt{-\langle 2-|4+5+6+7|2-\rangle}}, \\ A^{(2)}_{Wg,prod} &= \frac{e^2 V_{ud}^* V_{tb}}{2\sin^2\theta_W}\cdot\frac{(-i)2\sqrt{2}}{s_{567}-m_W^2}\frac{B^{(2)}_{Wg,prod}}{\sqrt{-\langle 2-|4+5+6+7|2-\rangle}}. \end{aligned} \tag{29}$$

As reference momentum for the massive spinor we have chosen $q = p_2$. As before all non-vanishing amplitudes have the helicity configuration (p_6^-, p_7^+). The non-vanishing amplitudes are

$$B^{(1)}_{Wg,prod}(p_4^+, p_5^+, p_8^-) = \frac{\langle 6-|4+5+7|2-\rangle}{\langle 65\rangle}\left(\frac{\langle 6-|4+5|7-\rangle}{\langle 45\rangle} + \frac{[74]\langle 6-|4+7|5-\rangle}{s_{467}-m^2}\right),$$

[2]For this channel the narrow width approximation has even been examined to one loop in [32].

$$
\begin{aligned}
B^{(1)}_{Wg,prod}(p_4^+,p_5^+,p_8^+) &= -\frac{m\langle 26\rangle}{\langle 65\rangle}\left(\frac{\langle 6-|4+5|7-\rangle}{\langle 45\rangle}+\frac{[74]\langle 6-|4+7|5-\rangle}{s_{467}-m^2}\right),\\
B^{(1)}_{Wg,prod}(p_4^+,p_5^-,p_8^-) &= \frac{[74]}{[54]\,(s_{467}-m^2)}\left(\langle 5-|4+6+7|2-\rangle[47]\langle 76\rangle+m^2[24]\langle 56\rangle\right),\\
B^{(1)}_{Wg,prod}(p_4^+,p_5^-,p_8^+) &= -\frac{m}{s_{467}-m^2}\frac{[47]}{[45]}\left(\langle 25\rangle\langle 67\rangle[74]+\langle 56\rangle\langle 2-|5+6+7|4-\rangle\right), \qquad (30)
\end{aligned}
$$

$$
\begin{aligned}
B^{(2)}_{Wg,prod}(p_4^+,p_5^+,p_8^-) &= \frac{\langle 6-|4+5+7|2-\rangle\langle 6-|5+7|4-\rangle}{\langle 56\rangle\langle 75\rangle},\\
B^{(2)}_{Wg,prod}(p_4^+,p_5^+,p_8^+) &= \frac{m\langle 62\rangle\langle 6-|5+7|4-\rangle}{\langle 56\rangle\langle 75\rangle},\\
B^{(2)}_{Wg,prod}(p_4^+,p_5^-,p_8^-) &= \frac{[74]\langle 2+|(4+5+6+7)(5+6)|7-\rangle}{[57][56]},\\
B^{(2)}_{Wg,prod}(p_4^+,p_5^-,p_8^+) &= \frac{m[47]\langle 2-|5+6|7-\rangle}{[57][56]}. \qquad (31)
\end{aligned}
$$

The helicity amplitudes for flavor-excitation and the s-channel process without the top decay

$$
0 \to t(p_8)+\bar{b}(p_4)+d(p_6)+\bar{u}(p_7), \qquad (32)
$$

are relatively simple and are given by

$$
A_{Wb,prod} = \delta_{84}\delta_{67}\frac{e^2V^*_{ud}V_{tb}}{2\sin^2\theta_W}\cdot\frac{2i}{s_{67}-m_W^2}\frac{B^{(1)}_{Wb,prod}}{\sqrt{-\langle 2-|4+6+7|2-\rangle}}. \qquad (33)
$$

As reference momentum for the massive spinor we have again chosen $q=p_2$. All helicity amplitudes have the configuration (p_6^-,p_7^+). The non-vanishing amplitudes are

$$
\begin{aligned}
B^{(1)}_{Wb,prod}(p_4^+,p_8^-) &= [47]\langle 6-|4+7|2-\rangle,\\
B^{(1)}_{Wb,prod}(p_4^+,p_8^+) &= m\langle 26\rangle[74]. \qquad (34)
\end{aligned}
$$

Finally, let us give the amplitude for the top decay

$$
t(p_8) \to \nu(p_1)+\bar{l}(p_2)+b(p_3). \qquad (35)
$$

With the choice $q=p_2$ as reference momentum for the top-spinor the only non-vanishing amplitude is

$$
A_{dec}(p_1^-,p_2^+,p_3^-,p_8^-) = \frac{e^2V^*_{tb}}{2\sin^2\theta_W}\frac{2i}{s_{12}-m_W^2}\langle 31\rangle\sqrt{\langle 2-|1+3|2-\rangle} \qquad (36)
$$

To implement the narrow top width approximation we keep in the amplitude only terms with a propagator $1/(p_8^2 - m^2 + im\Gamma)$ with Γ the inclusive top width. For the amplitude squared we obtain

$$\begin{aligned} |A|^2 &= \left| \sum_\lambda A_{dec}(..., p_8^\lambda) \frac{i}{p_8^2 - m^2 + im\Gamma} A_{prod}(..., p_8^\lambda) \right|^2 \\ &= |A_{dec}(..., p_8^-)|^2 \frac{1}{(p_8^2 - m^2)^2 + m^2\Gamma^2} |A_{prod}(..., p_8^-)|^2, \end{aligned} \tag{37}$$

because, with our choice of reference momentum for the massive spinor, $A_{dec}(..., p_8^+) = 0$. In the limit of vanishing top width the Breit-Wigner function in (37) reduces to a Dirac delta-function and we obtain for the squared amplitude

$$\frac{\pi}{m\Gamma} \delta(p_8^2 - m^2) |A_{dec}(..., p_8^-)|^2 |A_{prod}(..., p_8^-)|^2 \tag{38}$$

The full n-particle phase space may be factorized accordingly

$$d\phi_n(Q \to k_1, ..., k_n) = \frac{1}{2\pi} d\phi_{n-2}(Q \to p_8, k_4, ..., k_n) dp_8^2 d\phi_3(p_8 \to k_1, k_2, k_3), \tag{39}$$

with $n = 5$ for the W-gluon fusion and W-associated production, and $n = 4$ for flavor excitation and s-channel production. Note that

$$\int |A_{dec}(..., p_8^-)|^2 d\phi_3(p_8 \to k_1, k_2, k_3) = 2m\Gamma_{\nu\bar{l}b}. \tag{40}$$

Numerical results for the narrow top-width approximation are presented in the next section.

6 Numerical studies

As announced in the introduction, we consider for the purposes of numerical studies each subprocess separately. This is equivalent to assuming a hermetic detector with perfect momentum resolution capable of distinguishing these three processes.

Before describing our numerical studies we list our default choices for physical constants and parameters. For the masses and widths of the electroweak bosons we use $m_Z = 91.187$ GeV, $\Gamma_Z = 2.49$ GeV, $m_W = 80.41$ GeV and $\Gamma_W = 2.06$ GeV. For the top quark mass we use $m_t = 174$ GeV. The width of the top quark is then calculated as $\Gamma_t = 1.76$ GeV. We use the leading order expression for the running of the strong coupling constant:

$$\alpha_s(\mu) = \alpha_s(m_Z) \left[1 + \frac{\alpha_s(m_Z)}{4\pi} \beta_0 \ln \frac{\mu^2}{m_Z^2} \right]^{-1}, \tag{41}$$

where $\beta_0 = 11 - \frac{2}{3} N_f$ and $N_f = 5$. We use the CTEQ4L set for the parton densities [50] and we take therefore $\alpha_s(m_Z) = 0.132$. The running of the finestructure constant is taken

in account according to

$$\alpha(\mu) \;=\; \alpha(0)\left[1-\Delta\alpha(m_Z)-\frac{\alpha(0)}{3\pi}\left(\frac{20}{3}\ln\frac{\mu^2}{m_Z^2}-\frac{4}{15}\frac{(\mu^2-m_Z^2)}{m_t^2}\right)\right]^{-1}, \qquad (42)$$

with $\alpha(0) = 1/137.036$ and $\Delta\alpha(m_Z) = 0.059363$ ([51] - [54]). We consider p-$\bar{p}$ collisions with a center-of-mass energy $\sqrt{S} = 2.0$ TeV (Tevatron) and p-p collisions with a center-of-mass energy $\sqrt{S} = 14$ TeV (LHC). For the renormalization and factorization scale we use $\mu = \mu_F = m_t$. Jets are defined by the hadronic k_T-algorithm [55]: we first remove the charged lepton and the neutrino from the event, then we precluster all remaining particles and assign them to the beamjets or to the hard scattering process. Particles which are assigned to the hard scattering process are then clustered into jets. For the resolution variable of the hadronic k_T-algorithm we use

$$y_{ij} \;=\; 2\,\min\,(p_{Ti}^2, p_{Tj}^2)\,(\cosh(y_i-y_j)-\cos(\phi_i-\phi_j))\,, \qquad (43)$$

where p_{Ti} is the transverse momentum, y_i the rapidity and ϕ_i the polar angle of particle i. We recombine two particles using the E-scheme. For the preclustering we use $d_{cut} = (20\text{ GeV})^2$. The clustering is done with $y_{cut} = 0.9$. We have implemented the finite width of the W, Z-bosons and of the top quark by using the complex-mass scheme [56] which respects full gauge invariance and which therefore gives a consistent description of the finite-width effects in tree-level calculations. Thus, the masses m_W, m_Z and m_t in the partial amplitudes are replaced according to

$$m \;\to\; \sqrt{m^2 - i\Gamma m}. \qquad (44)$$

As a consequence the cosine squared of the Weinberg angle also becomes a complex number

$$\cos^2\theta_W \;=\; 1-\sin^2\theta_W = \frac{m_W^2 - i\Gamma_W m_W}{m_Z^2 - i\Gamma_Z m_Z}. \qquad (45)$$

We give our results for single-top production only. Furthermore we concentrate most of our studies on the Tevatron. LHC kinematics reweights the various processes among each other, the amount of which is not so much our concern in this paper (see [16] e.g.).

Although we do not combine the partonic subprocesses, and rather examine them individually, we wish to define their final state in a semi-realistic manner. Specifically, we keep the parton apart in phase space by means of a jet algorithm (this includes in particular, for the W-gluon channel, the beam and the $\bar{b}$ jet). However, we do assume perfect b-tagging, and no mistagging.

The inclusion of single-antitop production will multiply the cross section by a factor of two at the Tevatron. This is not the case at the LHC, which is a proton-proton collider. The numerical results are for one light lepton species only, e.g. $\bar{l} = e^+$ and $\nu = \nu_e$. The inclusion of the muon-channel multiplies every result by two.

For W-gluon fusion we require three jets, two of them b-tagged, for flavor-excitation two

Tevatron	σ_{tot}	$\lvert m_{\nu\bar{l}b} - m_t\rvert < 20$ GeV	narrow width
Wg	15.0 ± 0.4 fb	14.3 ± 0.3 fb	14.5 ± 0.1 fb
Wb	87 ± 1 fb	85 ± 2 fb	87 ± 1 fb
$q\bar{q}$	46 ± 1 fb	32.3 ± 0.3 fb	29.0 ± 0.2 fb

Table 1: Numerical results for Tevatron at 2 TeV.

LHC	σ_{tot}	$\lvert m_{\nu\bar{l}b} - m_t\rvert < 20$ GeV	narrow width
Wg	4.6 ± 0.2 pb	4.5 ± 0.4 pb	4.6 ± 0.1 pb
Wb	13.1 ± 0.3 pb	13.0 ± 0.4 pb	13.3 ± 0.1 pb
$q\bar{q}$	685 ± 19 fb	479 ± 16 fb	432 ± 4 fb

Table 2: Numerical results for the LHC at 14 TeV.

jets with one b-tag, whereas for the s-channel process we require two b-tagged jets. For simplicity we assume a b-tagging efficiency of 100%, and that we know the longitudinal momentum component of the neutrino[3].

In Table 1 we give the numerical results for the total cross section with the cuts described above for W-gluon fusion, flavor-excitation and s-channel process at the Tevatron (first column). In the second column we required in addition that the invariant mass of the decay products of the top reconstruct to within 20 GeV to the top quark mass. The third column contains the results in the narrow width approximation. Table 2 shows the corresponding results for the LHC. From Table 1 and Table 2 we see that the narrow width approximation describes the cross section very well for W-gluon fusion and flavor excitation. The approximation is less satisfactory for s-channel process. Here non-resonant terms seem to give a more sizeable contribution. This can also be seen in Fig. 4, which shows the distribution in the invariant mass $m_{\nu\bar{l}b}$ for W-gluon fusion and the s-channel process at the Tevatron.

In Fig. 5 we show for the W-gluon fusion process at the Tevatron the distribution of the pseudorapidities for the $\bar{b}$-quark, the b-quark and the light quark q. The distribution for the $\bar{b}$-quark is slightly peaked in the backward region, the b-quark is almost central and the light quark goes dominantly in the forward region. Note that the jet algorithm suppresses $\bar{b}$'s at sizeable negative pseudo-rapidities. These distributions essentially agree with Fig. 7 in [6] and Fig. 8 in [12].

In W-gluon fusion or flavor excitation the produced top quark is highly polarized along the direction of the $\bar{d}$-quark [14, 18]. Furthermore the cross section at the Tevatron receives the dominant contribution from the configuration where the u-quark is in the initial state

[3]E.g. from imposing the W mass constraint on the neutrino plus lepton invariant mass [4].

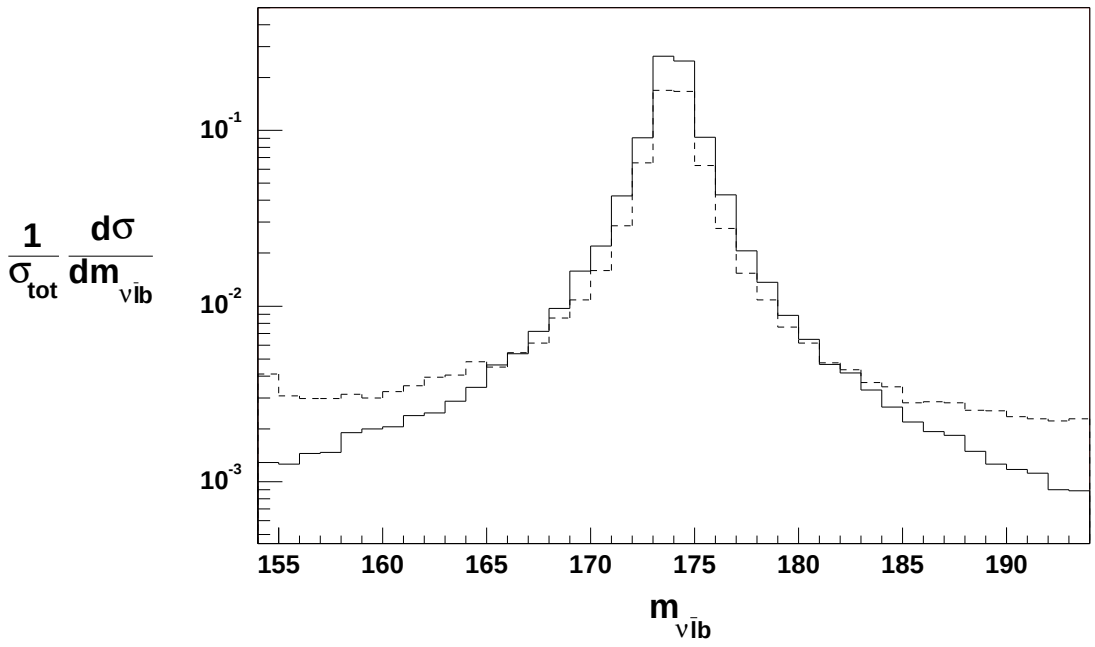

Figure 4: *The normalized $m_{\nu\bar{l}b}$ distribution for W-gluon fusion (solid) and the s-channel process (dashed) at the Tevatron.*

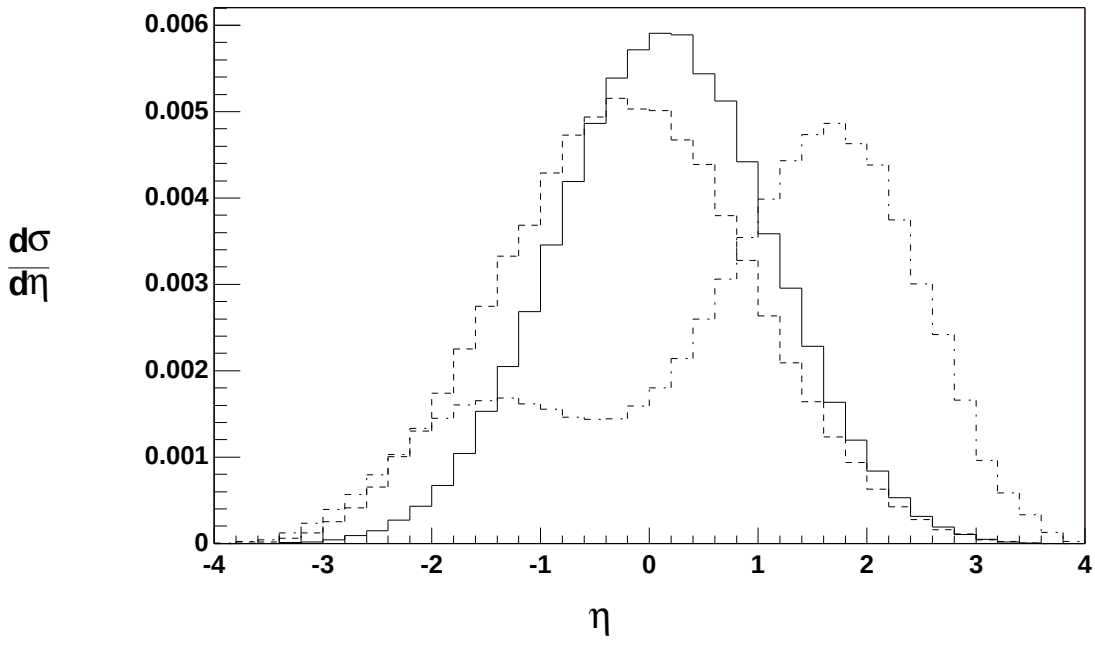

Figure 5: *The pseudo-rapidity distribution for W-gluon fusion of the $\bar{b}$-quark (dashed), the b-quark (solid) and the light quark q (dot-dashed) at the Tevatron.*

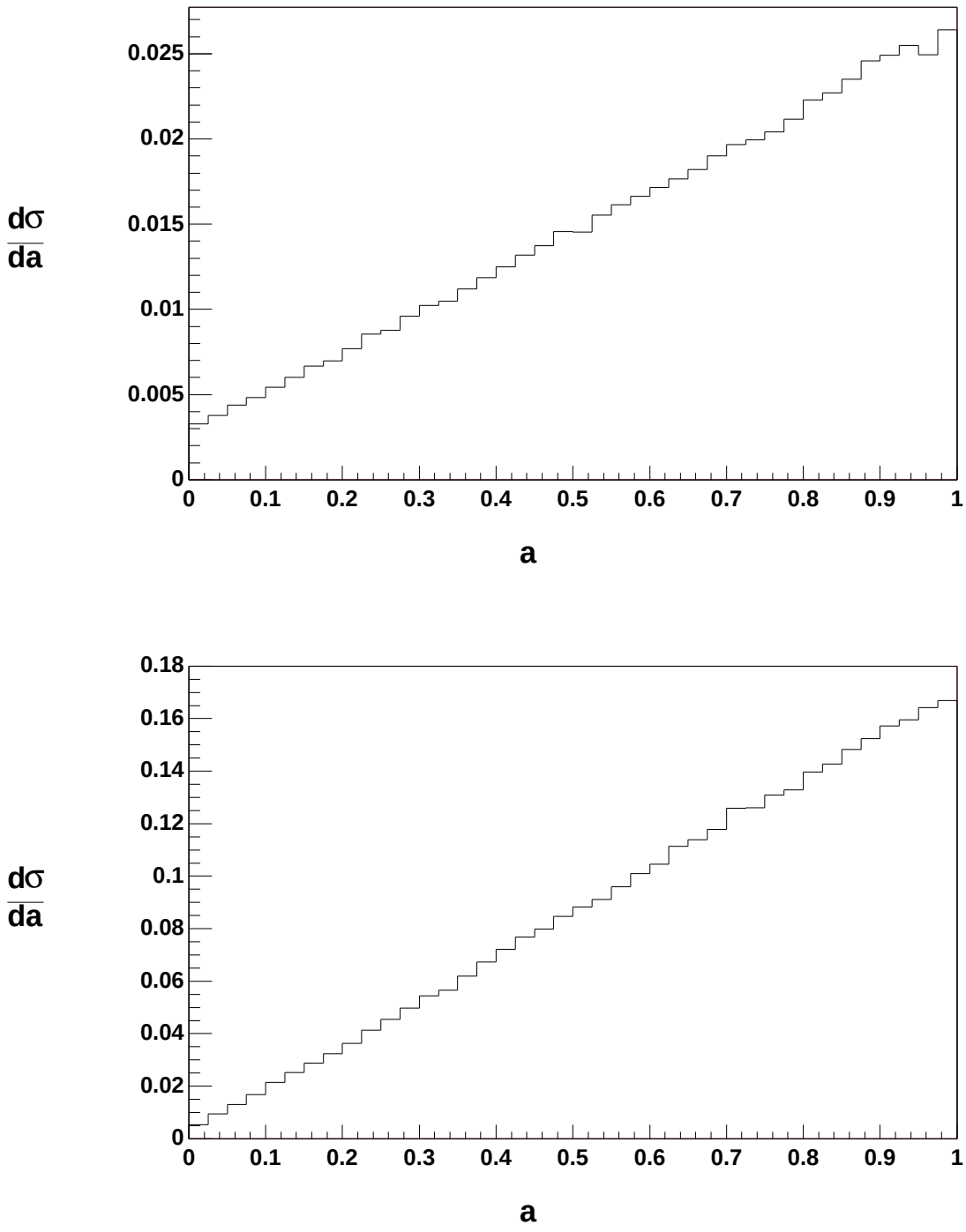

Figure 6: *The distribution for the angular correlation a for W-gluon fusion (top) and flavor excitation (bottom) at the Tevatron.*

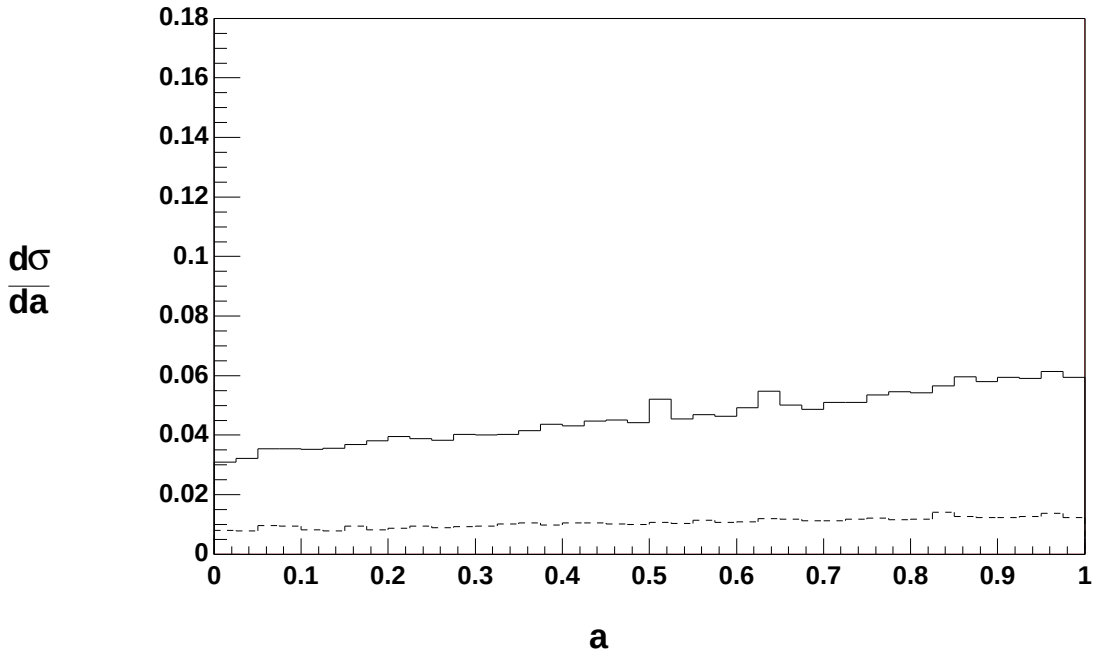

Figure 7: *The distribution for the angular correlation a for the "QCD + Weak" background to flavor excitation at the Tevatron. We show the distribution with (dashed) and without (solid) a cut on the invariant mass* $|m_{\nu\bar{l}b} - m_t| < 20\ GeV$.

and the $\bar{d}$-quark in the final state, which in turn produces the non-b tagged jet q. One considers therefore the variable

$$a = \frac{1}{2}\left(1 + \cos\theta_{q\bar{l}}\right) \tag{46}$$

where $\theta_{q\bar{l}}$ is the angle between the non-b tagged jet and the charged lepton in the rest frame of $p_\nu + p_{\bar{l}} + p_b$ [57]. (If a top is produced, $p_\nu + p_{\bar{l}} + p_b$ corresponds to its four-momentum.) For the angular correlation of a decaying top quark one has [58]

$$\frac{d\sigma}{da} = \sigma\left(2Pa + (1-P)\right), \tag{47}$$

where P is the polarization of the top quark along the spin axis defined by the spectator jet q. For a 100% polarized top quark one has therefore $d\sigma/da \sim a$. Fig. 6 shows that this relation is fullfilled to a very good approximation for flavour excitation. For W-gluon fusion we obtain the polarization along the spectator jet axis from the value at $a = 0$:

$$P = 1 - \frac{1}{\sigma}\frac{d\sigma}{da}\bigg|_{a=0} \tag{48}$$

With the total cross section from Table 1 we find $P = 77\%$ for W-gluon fusion. The background is expected to give a flat distribution. For flavor excitation we show in fact the result for the "QCD + Weak" background process in Fig. 7, discussed below (24), whose a dependence after imposing a cut on the invariant mass $m_{\nu\bar{l}b}$ is flat, as expected. Our result is similar to that shown in Fig. 5 of [16], which shows the same linear correlation of the signal (which is somewhat different from ours by employing a vetoed $\bar{b}$ jet), and shows the (flat) a dependence of their more extensively treated background as well.

We suggest that this clear correlation may provide an alternative and attractive way to infer the visible W-gluon fusion or flavor excitation cross section (defined here through the criteria given above) for single-top production from the slope of the distribution. The slope is given by

$$2P_{signal}\sigma_{signal} + 2P_{background}\sigma_{background} \tag{49}$$

Assuming that $P_{background}\sigma_{background}$ is small and that P_{signal} may reliable be estimated from theory the visible cross section for the signal can be inferred from the slope by measuring two or more points of the a distribution and extrapolating the distribution to a straight line. Although in principle of course any distribution may serve to infer the corresponding inclusive cross section, the a distribution seems particularly attractive due to its simple shape.

7 Conclusions

We have presented the complete $O(g_w^4)$ and $O(gg_w^4)$ helicity amplitudes for processes whose final state results from the hadroproduction and semileptonic decay of a single top.

As only a small subset of graphs actually contain a top quark line in each process, we have examined, for three of these processes, to what extent the top quark dominates, and verified that for each process the top quark presence is manifested by a clear peak in the $m_{\nu\bar{l}b}$ distribution. We have studied various kinematic distribution of final state particles, and verified the correlation of the lepton angular distribution with the top quark polarization [14, 16, 18]. The actual identification of a single top signal is a matter of careful definition, requiring full use of the kinematic and flavor characteristics of the final state, and a proper determination of the acceptance and background [16, 17, 30]. In an idealized analyses, we have thus verified that the sensitivity of the full amplitudes to top quark mass, charged-current coupling strength and handedness are preserved in these amplitudes, even though most diagrams that contribute to them do not contain a top quark.

Acknowledgments

We would like to thank Brian Harris and Zack Sullivan for illuminating discussions. This work is part of the research program of the Foundation for Fundamental Research of Matter (FOM) and the National Organization for Scientific Research (NWO).

A Helicity amplitudes for W-gluon fusion

We give here the helicity amplitudes for the configurations (p_3^-, p_4^+, p_5^+), (p_3^-, p_4^+, p_5^-), (p_3^+, p_4^-, p_5^+) and (p_3^+, p_4^-, p_5^-).

$$A_{Wg}^{(1,1)} = \frac{4\sqrt{2}iB_{Wg}^{(1,1)}}{(s_{12}-m_W^2)(s_{67}-m_W^2)}, \tag{50}$$

$$\begin{aligned}
B_{Wg}^{(1,1)}(p_3^-,p_4^+,p_5^+) &= \frac{1}{s_{123}-m^2}\frac{\langle 31\rangle}{\langle 35\rangle}\left(\frac{\langle 3-|4+5|7-\rangle\langle 6-|1+3|2-\rangle}{\langle 54\rangle}\right.\\
&\quad\left.+\frac{[47]}{s_{467}-m^2}\Big([21]\langle 13\rangle\langle 6-|4+7|5-\rangle - m^2[25]\langle 36\rangle\Big)\right),\\
B_{Wg}^{(1,1)}(p_3^-,p_4^+,p_5^-) &= \frac{1}{s_{467}-m^2}\frac{[74]}{[54]}\left(\frac{\langle 1-|3+5|4-\rangle\langle 6-|4+7|2-\rangle}{[35]}\right.\\
&\quad\left.+\frac{\langle 13\rangle}{s_{123}-m^2}\Big(\langle 67\rangle[74]\langle 5-|1+3|2-\rangle - m^2\langle 56\rangle[24]\Big)\right),\\
B_{Wg}^{(1,1)}(p_3^+,p_4^-,p_5^+) &= 0,\\
B_{Wg}^{(1,1)}(p_3^+,p_4^-,p_5^-) &= 0,
\end{aligned}$$

$$A_{Wg}^{(1,2)} = \frac{4\sqrt{2}iB_{Wg}^{(1,2)}}{(s_{12}-m_W^2)s_{345}s_{127}}, \tag{51}$$

$$
\begin{aligned}
B^{(1,2)}_{Wg}(p_3^-,p_4^+,p_5^+) &= \frac{\langle 36\rangle}{\langle 54\rangle\langle 35\rangle}[27]\langle 1-|(2+7)(4+5)|3+\rangle,\\
B^{(1,2)}_{Wg}(p_3^-,p_4^+,p_5^-) &= \frac{[27]}{[54][53]}\langle 6-|3+5|4-\rangle\langle 1-|2+7|4-\rangle,\\
B^{(1,2)}_{Wg}(p_3^+,p_4^-,p_5^+) &= \frac{\langle 64\rangle}{\langle 45\rangle\langle 35\rangle}[27]\langle 4-|(3+5)(2+7)|1+\rangle,\\
B^{(1,2)}_{Wg}(p_3^+,p_4^-,p_5^-) &= \frac{[27]}{[45][53]}\langle 1-|2+7|3-\rangle\langle 6-|4+5|3-\rangle,
\end{aligned}
$$

$$
A^{(1,3)}_{Wg} = \frac{4\sqrt{2}iB^{(1,3)}_{Wg}}{(s_{12}-m_W^2)s_{345}s_{126}}, \tag{52}
$$

$$
\begin{aligned}
B^{(1,3)}_{Wg}(p_3^-,p_4^+,p_5^+) &= \frac{\langle 61\rangle}{\langle 45\rangle\langle 35\rangle}\langle 3-|1+6|2-\rangle\langle 3-|4+5|7-\rangle,\\
B^{(1,3)}_{Wg}(p_3^-,p_4^+,p_5^-) &= \frac{[47]}{[54][53]}\langle 61\rangle\langle 4+|(3+5)(1+6)|2-\rangle,\\
B^{(1,3)}_{Wg}(p_3^+,p_4^-,p_5^+) &= \frac{\langle 61\rangle}{\langle 45\rangle\langle 53\rangle}\langle 4-|1+6|2-\rangle\langle 4-|3+5|7-\rangle,\\
B^{(1,3)}_{Wg}(p_3^+,p_4^-,p_5^-) &= \frac{[37]}{[54][53]}\langle 61\rangle\langle 2+|(1+6)(4+5)|3-\rangle,
\end{aligned}
$$

$$
A^{(1,4)}_{Wg} = \frac{4\sqrt{2}iB^{(1,4)}_{Wg}}{(s_{12}-m_W^2)(s_{67}-m_W^2)s_{345}}, \tag{53}
$$

$$
\begin{aligned}
B^{(1,4)}_{Wg}(p_3^-,p_4^+,p_5^+) &= \frac{1}{\langle 54\rangle\langle 35\rangle}\left(\langle 31\rangle\langle 6-|1+2|7-\rangle\langle 3-|4+5|2-\rangle\right.\\
&\quad \left.-\langle 36\rangle\langle 1-|6+7|2-\rangle\langle 3-|4+5|7-\rangle+\langle 16\rangle[72]\langle 3-|(6+7)(4+5)|3+\rangle\right),\\
B^{(1,4)}_{Wg}(p_3^-,p_4^+,p_5^-) &= \frac{1}{[53][54]}\left([24]\langle 6-|1+2|7-\rangle\langle 1-|3+5|4-\rangle\right.\\
&\quad \left.-[74]\langle 1-|6+7|2-\rangle\langle 6-|3+5|4-\rangle-[72]\langle 16\rangle\langle 4+|(6+7)(3+5)|4-\rangle\right),\\
B^{(1,4)}_{Wg}(p_3^+,p_4^-,p_5^+) &= \frac{1}{\langle 45\rangle\langle 53\rangle}\left(\langle 14\rangle\langle 6-|1+2|7-\rangle\langle 4-|3+5|2-\rangle\right.\\
&\quad \left.-\langle 64\rangle\langle 1-|6+7|2-\rangle\langle 4-|3+5|7-\rangle+\langle 16\rangle[72]\langle 4-|(3+5)(6+7)|4+\rangle\right),\\
B^{(1,4)}_{Wg}(p_3^+,p_4^-,p_5^-) &= \frac{1}{[54][53]}\left([32]\langle 6-|1+2|7-\rangle\langle 1-|4+5|3-\rangle\right.\\
&\quad \left.-[37]\langle 1-|6+7|2-\rangle\langle 6-|4+5|3-\rangle+\langle 16\rangle[72]\langle 3+|(6+7)(4+5)|3-\rangle\right),
\end{aligned}
$$

$$
A^{(1,5)}_{Wg} = \frac{4\sqrt{2}iB^{(1,5)}_{Wg}}{(s_{67}-m_W^2)s_{345}s_{167}}, \tag{54}
$$

$$
\begin{aligned}
B_{Wg}^{(1,5)}(p_3^-,p_4^+,p_5^+) &= \frac{\langle 16\rangle}{\langle 35\rangle\langle 45\rangle}\langle 3-|1+6|7-\rangle\langle 3-|4+5|2-\rangle,\\
B_{Wg}^{(1,5)}(p_3^-,p_4^+,p_5^-) &= \frac{[24]}{[45][35]}\langle 16\rangle\langle 7+|(1+6)(3+5)|4-\rangle,\\
B_{Wg}^{(1,5)}(p_3^+,p_4^-,p_5^+) &= -\frac{\langle 16\rangle}{\langle 35\rangle\langle 45\rangle}\langle 4-|1+6|7-\rangle\langle 4-|3+5|2-\rangle,\\
B_{Wg}^{(1,5)}(p_3^+,p_4^-,p_5^-) &= -\frac{[23]}{[35][45]}\langle 16\rangle\langle 7+|(1+6)(4+5)|3-\rangle,
\end{aligned}
$$

$$
A_{Wg}^{(1,6)} = \frac{4\sqrt{2}iB_{Wg}^{(1,6)}}{(s_{67}-m_W^2)s_{345}s_{267}}, \tag{55}
$$

$$
\begin{aligned}
B_{Wg}^{(1,6)}(p_3^-,p_4^+,p_5^+) &= \frac{\langle 13\rangle}{\langle 35\rangle\langle 45\rangle}[27]\langle 3-|(4+5)(2+7)|6+\rangle,\\
B_{Wg}^{(1,6)}(p_3^-,p_4^+,p_5^-) &= -\frac{[27]}{[35][45]}\langle 1-|3+5|4-\rangle\langle 6-|2+7|4-\rangle,\\
B_{Wg}^{(1,6)}(p_3^+,p_4^-,p_5^+) &= -\frac{\langle 14\rangle}{\langle 35\rangle\langle 45\rangle}[27]\langle 4-|(3+5)(2+7)|6+\rangle,\\
B_{Wg}^{(1,6)}(p_3^+,p_4^-,p_5^-) &= \frac{[27]}{[35][45]}\langle 1-|4+5|3-\rangle\langle 6-|2+7|3-\rangle,
\end{aligned}
$$

$$
A_{Wg}^{(2,1)} = \frac{4\sqrt{2}iB_{Wg}^{(2,1)}}{(s_{12}-m_W^2)(s_{567}-m_W^2)(s_{123}-m^2)}, \tag{56}
$$

$$
\begin{aligned}
B_{Wg}^{(2,1)}(p_3^-,p_4^+,p_5^+) &= \frac{\langle 31\rangle}{\langle 65\rangle\langle 75\rangle}\langle 6-|1+3|2-\rangle\langle 6-|5+7|4-\rangle,\\
B_{Wg}^{(2,1)}(p_3^-,p_4^+,p_5^-) &= \frac{[47]}{[57][56]}\langle 31\rangle\langle 2+|(1+3)(5+6)|7-\rangle,\\
B_{Wg}^{(2,1)}(p_3^+,p_4^-,p_5^+) &= 0,\\
B_{Wg}^{(2,1)}(p_3^+,p_4^-,p_5^-) &= 0,
\end{aligned}
$$

$$
A_{Wg}^{(2,2)} = \frac{4\sqrt{2}iB_{Wg}^{(2,2)}}{(s_{12}-m_W^2)s_{34}}, \tag{57}
$$

$$
\begin{aligned}
&B_{Wg}^{(2,2)}(p_3^-,p_4^+,p_5^+) =\\
&\quad\frac{1}{s_{346}}\frac{\langle 63\rangle}{\langle 65\rangle}\left(\frac{\langle 1-|3+6|4-\rangle\langle 6-|5+7|2-\rangle}{\langle 57\rangle}-\frac{[43]\langle 36\rangle}{s_{127}}[27]\langle 1-|2+7|5-\rangle\right),
\end{aligned}
$$

$$
\begin{aligned}
&B^{(2,2)}_{Wg}(p_3^-,p_4^+,p_5^-) = \\
&\quad -\frac{1}{s_{127}}\frac{[27]}{[57]}\left(\frac{\langle 3-|5+6|7-\rangle\langle 1-|2+7|4-\rangle}{[56]}+\frac{\langle 63\rangle\langle 12\rangle[27]\langle 5-|3+6|4-\rangle}{s_{346}}\right),\\
&B^{(2,2)}_{Wg}(p_3^+,p_4^-,p_5^+) = \\
&\quad \frac{1}{s_{346}}\frac{\langle 64\rangle}{\langle 65\rangle}\left(\frac{\langle 1-|4+6|3-\rangle\langle 6-|5+7|2-\rangle}{\langle 57\rangle}-\frac{[34]\langle 46\rangle}{s_{127}}[27]\langle 1-|2+7|5-\rangle\right),\\
&B^{(2,2)}_{Wg}(p_3^+,p_4^-,p_5^-) = \\
&\quad -\frac{1}{s_{127}}\frac{[27]}{[57]}\left(\frac{\langle 4-|5+6|7-\rangle\langle 1-|2+7|3-\rangle}{[56]}+\frac{\langle 64\rangle\langle 12\rangle[27]\langle 5-|4+6|3-\rangle}{s_{346}}\right),
\end{aligned}
$$

$$
A^{(2,3)}_{Wg} \;=\; \frac{4\sqrt{2}iB^{(2,3)}_{Wg}}{(s_{12}-m_W^2)s_{34}}, \tag{58}
$$

$$
\begin{aligned}
&B^{(2,3)}_{Wg}(p_3^-,p_4^+,p_5^+) = \\
&\quad \frac{1}{s_{126}}\frac{\langle 61\rangle}{\langle 65\rangle}\left(\frac{\langle 3-|1+6|2-\rangle\langle 6-|5+7|4-\rangle}{\langle 57\rangle}-\frac{[21]\langle 16\rangle[47]\langle 3-|4+7|5-\rangle}{s_{347}}\right),\\
&B^{(2,3)}_{Wg}(p_3^-,p_4^+,p_5^-) = \\
&\quad -\frac{1}{s_{347}}\frac{[47]}{[57]}\left(\frac{\langle 1-|5+6|7-\rangle\langle 3-|4+7|2-\rangle}{[56]}-\frac{\langle 61\rangle[74]\langle 34\rangle\langle 5-|1+6|2-\rangle}{s_{126}}\right),\\
&B^{(2,3)}_{Wg}(p_3^+,p_4^-,p_5^+) = \\
&\quad \frac{1}{s_{126}}\frac{\langle 61\rangle}{\langle 65\rangle}\left(\frac{\langle 4-|1+6|2-\rangle\langle 6-|5+7|3-\rangle}{\langle 57\rangle}-\frac{[21]\langle 16\rangle[37]\langle 4-|3+7|5-\rangle}{s_{347}}\right),\\
&B^{(2,3)}_{Wg}(p_3^+,p_4^-,p_5^-) = \\
&\quad -\frac{1}{s_{347}}\frac{[37]}{[57]}\left(\frac{\langle 1-|5+6|7-\rangle\langle 4-|3+7|2-\rangle}{[56]}-\frac{\langle 61\rangle[73]\langle 43\rangle\langle 5-|1+6|2-\rangle}{s_{126}}\right),
\end{aligned}
$$

$$
A^{(2,4)}_{Wg} \;=\; \frac{4\sqrt{2}iB^{(2,4)}_{Wg}}{(s_{12}-m_W^2)(s_{567}-m_W^2)s_{34}}, \tag{59}
$$

$$
\begin{aligned}
&B^{(2,4)}_{Wg}(p_3^-,p_4^+,p_5^+) = -\frac{1}{\langle 75\rangle\langle 65\rangle}\left(\langle 63\rangle\langle 1-|3+4|2-\rangle\langle 6-|5+7|4-\rangle\right.\\
&\quad \left.-\langle 61\rangle\langle 3-|1+2|4-\rangle\langle 6-|5+7|2-\rangle+\langle 13\rangle[42]\langle 6-|(1+2)(5+7)|6+\rangle\right),\\
&B^{(2,4)}_{Wg}(p_3^-,p_4^+,p_5^-) = -\frac{1}{[57][65]}\left([47]\langle 1-|3+4|2-\rangle\langle 3-|5+6|7-\rangle\right.\\
&\quad \left.-[27]\langle 3-|1+2|4-\rangle\langle 1-|5+6|7-\rangle+[42]\langle 13\rangle\langle 7+|(5+6)(1+2)|7-\rangle\right),
\end{aligned}
$$

$$B_{Wg}^{(2,4)}(p_3^+,p_4^-,p_5^+) = -\frac{1}{\langle 75\rangle\langle 65\rangle}\left(\langle 64\rangle\langle 1-|3+4|2-\rangle\langle 6-|5+7|3-\rangle\right.$$
$$\left.-\langle 61\rangle\langle 4-|1+2|3-\rangle\langle 6-|5+7|2-\rangle+\langle 14\rangle[32]\langle 6-|(1+2)(5+7)|6+\rangle\right),$$
$$B_{Wg}^{(2,4)}(p_3^+,p_4^-,p_5^-) = -\frac{1}{[57][65]}\left([37]\langle 1-|3+4|2-\rangle\langle 4-|5+6|7-\rangle\right.$$
$$\left.-[27]\langle 4-|1+2|3-\rangle\langle 1-|5+6|7-\rangle+[32]\langle 14\rangle\langle 7+|(5+6)(1+2)|7-\rangle\right),$$

$$A_{Wg}^{(2,5)} = \frac{4\sqrt{2}iB_{Wg}^{(2,5)}}{(s_{567}-m_W^2)s_{34}s_{234}}, \tag{60}$$

$$\begin{aligned}
B_{Wg}^{(2,5)}(p_3^-,p_4^+,p_5^+) &= \frac{\langle 16\rangle}{\langle 56\rangle\langle 57\rangle}[24]\langle 6-|(5+7)(2+4)|3+\rangle,\\
B_{Wg}^{(2,5)}(p_3^-,p_4^+,p_5^-) &= -\frac{[24]}{[56][57]}\langle 1-|5+6|7-\rangle\langle 3-|2+4|7-\rangle,\\
B_{Wg}^{(2,5)}(p_3^+,p_4^-,p_5^+) &= \frac{\langle 16\rangle}{\langle 56\rangle\langle 57\rangle}[23]\langle 6-|(5+7)(2+3)|4+\rangle,\\
B_{Wg}^{(2,5)}(p_3^+,p_4^-,p_5^-) &= -\frac{[23]}{[56][57]}\langle 1-|5+6|7-\rangle\langle 4-|2+3|7-\rangle,
\end{aligned}$$

$$A_{Wg}^{(2,6)} = \frac{4\sqrt{2}iB_{Wg}^{(2,6)}}{(s_{567}-m_W^2)s_{34}s_{134}}, \tag{61}$$

$$\begin{aligned}
B_{Wg}^{(2,6)}(p_3^-,p_4^+,p_5^+) &= \frac{\langle 13\rangle}{\langle 56\rangle\langle 57\rangle}\langle 6-|1+3|4-\rangle\langle 6-|5+7|2-\rangle,\\
B_{Wg}^{(2,6)}(p_3^-,p_4^+,p_5^-) &= \frac{[27]}{[56][57]}\langle 13\rangle\langle 4+|(1+3)(5+6)|7-\rangle,\\
B_{Wg}^{(2,6)}(p_3^+,p_4^-,p_5^+) &= \frac{\langle 14\rangle}{\langle 56\rangle\langle 57\rangle}\langle 6-|1+4|3-\rangle\langle 6-|5+7|2-\rangle,\\
B_{Wg}^{(2,6)}(p_3^+,p_4^-,p_5^-) &= \frac{[27]}{[56][57]}\langle 14\rangle\langle 3+|(1+4)(5+6)|7-\rangle.
\end{aligned}$$

B Helicity amplitudes for flavor excitation and the s-channel

We give here the helicity amplitudes for the configurations (p_3^-,p_4^+), and (p_3^+,p_4^-).

$$A_{Wb}^{(1,1)} = \frac{-4iB_{Wb}^{(1,1)}}{(s_{12}-m_W^2)(s_{67}-m_W^2)(s_{123}-m^2)}, \tag{62}$$

$$
\begin{aligned}
B^{(1,1)}_{Wb}(p_3^-,p_4^+) &= \langle 31\rangle[74]\langle 6-|1+3|2-\rangle,\\
B^{(1,1)}_{Wb}(p_3^+,p_4^-) &= 0,
\end{aligned}
$$

$$
A^{(1,2)}_{Wb} = \frac{-4iB^{(1,2)}_{Wb}}{(s_{12}-m_W^2)s_{34}s_{346}}, \tag{63}
$$

$$
\begin{aligned}
B^{(1,2)}_{Wb}(p_3^-,p_4^+) &= \langle 63\rangle[27]\langle 1-|3+6|4-\rangle,\\
B^{(1,2)}_{Wb}(p_3^+,p_4^-) &= \langle 64\rangle[27]\langle 1-|4+6|3-\rangle,
\end{aligned}
$$

$$
A^{(1,3)}_{Wb} = \frac{-4iB^{(1,3)}_{Wb}}{(s_{12}-m_W^2)s_{34}s_{126}}, \tag{64}
$$

$$
\begin{aligned}
B^{(1,3)}_{Wb}(p_3^-,p_4^+) &= \langle 61\rangle[47]\langle 3-|1+6|2-\rangle,\\
B^{(1,3)}_{Wb}(p_3^+,p_4^-) &= \langle 61\rangle[37]\langle 4-|1+6|2-\rangle,
\end{aligned}
$$

$$
A^{(1,4)}_{Wb} = \frac{-4iB^{(1,4)}_{Wb}}{(s_{12}-m_W^2)(s_{67}-m_W^2)s_{34}}, \tag{65}
$$

$$
\begin{aligned}
B^{(1,4)}_{Wb}(p_3^-,p_4^+) &= -\langle 63\rangle[47]\langle 1-|6+7|2-\rangle - \langle 13\rangle[42]\langle 6-|3+4|7-\rangle\\
&\quad -\langle 61\rangle[27]\langle 3-|1+2|4-\rangle,\\
B^{(1,4)}_{Wb}(p_3^+,p_4^-) &= -\langle 64\rangle[37]\langle 1-|6+7|2-\rangle - \langle 14\rangle[32]\langle 6-|3+4|7-\rangle\\
&\quad -\langle 61\rangle[27]\langle 4-|1+2|3-\rangle,
\end{aligned}
$$

$$
A^{(1,5)}_{Wb} = \frac{-4iB^{(1,5)}_{Wb}}{(s_{67}-m_W^2)s_{34}s_{167}}, \tag{66}
$$

$$
\begin{aligned}
B^{(1,5)}_{Wb}(p_3^-,p_4^+) &= \langle 16\rangle[42]\langle 3-|1+6|7-\rangle,\\
B^{(1,5)}_{Wb}(p_3^+,p_4^-) &= \langle 16\rangle[32]\langle 4-|1+6|7-\rangle,
\end{aligned}
$$

$$
A^{(1,6)}_{Wb} = \frac{-4iB^{(1,6)}_{Wb}}{(s_{67}-m_W^2)s_{34}s_{134}}, \tag{67}
$$

$$
\begin{aligned}
B^{(1,6)}_{Wb}(p_3^-,p_4^+) &= \langle 13\rangle[72]\langle 6-|1+3|4-\rangle,\\
B^{(1,6)}_{Wb}(p_3^+,p_4^-) &= \langle 14\rangle[72]\langle 6-|1+4|3-\rangle.
\end{aligned}
$$

References

[1] D0, S. Abachi *et al.*, Phys. Rev. Lett. **74**, 2632 (1995), hep-ex/9503003.

[2] CDF, F. Abe *et al.*, Phys. Rev. Lett. **74**, 2626 (1995), hep-ex/9503002.

[3] D. A. Dicus and S. S. D. Willenbrock, Phys. Rev. **D34**, 148 (1986).

[4] C. P. Yuan, Phys. Rev. **D41**, 42 (1990).

[5] S. Cortese and R. Petronzio, Phys. Lett. **B253**, 494 (1991).

[6] R. K. Ellis and S. Parke, Phys. Rev. **D46**, 3785 (1992).

[7] G. Bordes and B. van Eijk, Z. Phys. **C57**, 81 (1993).

[8] G. Bordes and B. van Eijk, Nucl. Phys. **B435**, 23 (1995).

[9] D. O. Carlson and C. P. Yuan, (1995), hep-ph/9509208.

[10] T. Stelzer and S. Willenbrock, Phys. Lett. **B357**, 125 (1995), hep-ph/9505433.

[11] M. C. Smith and S. Willenbrock, Phys. Rev. **D54**, 6696 (1996), hep-ph/9604223.

[12] A. P. Heinson, A. S. Belyaev, and E. E. Boos, Phys. Rev. **D56**, 3114 (1997), hep-ph/9612424.

[13] T. Stelzer, Z. Sullivan, and S. Willenbrock, Phys. Rev. **D56**, 5919 (1997), hep-ph/9705398.

[14] G. Mahlon and S. Parke, Phys. Rev. **D55**, 7249 (1997), hep-ph/9611367.

[15] T. Tait and C. P. Yuan, (1997), hep-ph/9710372.

[16] T. Stelzer, Z. Sullivan, and S. Willenbrock, Phys. Rev. **D58**, 094021 (1998), hep-ph/9807340.

[17] A. S. Belyaev, E. E. Boos, and L. V. Dudko, Phys. Rev. **D59**, 075001 (1999), hep-ph/9806332.

[18] G. Mahlon and S. Parke, (1999), hep-ph/9912458.

[19] T. M. P. Tait, Phys. Rev. **D61**, 034001 (2000), hep-ph/9909352.

[20] D. O. Carlson, E. Malkawi, and C. P. Yuan, Phys. Lett. **B337**, 145 (1994), hep-ph/9405277.

[21] D. Atwood, S. Bar-Shalom, G. Eilam, and A. Soni, Phys. Rev. **D54**, 5412 (1996), hep-ph/9605345.

[22] A. Datta, P. J. O'Donnell, Z. H. Lin, X. Zhang, and T. Huang, (2000), hep-ph/0001059.

[23] A. Datta and X. Zhang, Phys. Rev. **D55**, 2530 (1997), hep-ph/9611247.

[24] A. Datta, J. M. Yang, B.-L. Young, and X. Zhang, Phys. Rev. **D56**, 3107 (1997), hep-ph/9704257.

[25] C.-S. Li, R. J. Oakes, J.-M. Yang, and H.-Y. Zhou, Phys. Rev. **D57**, 2009 (1998), hep-ph/9706412.

[26] C. S. Li, R. J. Oakes, and J. M. Yang, Phys. Rev. **D55**, 5780 (1997), hep-ph/9611455.

[27] C. S. Li, R. J. Oakes, and J. M. Yang, Phys. Rev. **D55**, 1672 (1997), hep-ph/9608460.

[28] E. H. Simmons, Phys. Rev. **D55**, 5494 (1997), hep-ph/9612402.

[29] G. ru Lu, Y. gang Cao, J. shu Huang, J. de Zhang, and Z. jun Xiao, (1997), hep-ph/9701406.

[30] CDF, Y.-C. Liu, To be published in the proceedings of 13th Topical Conference on Hadron Collider Physics, Mumbai, India, 14-20 Jan 1999.

[31] I. I. Y. Bigi, Y. L. Dokshitzer, V. Khoze, J. Kuhn, and P. Zerwas, Phys. Lett. **B181**, 157 (1986).

[32] R. Pittau, Phys. Lett. **B386**, 397 (1996), hep-ph/9603265.

[33] G. Mahlon and S. Parke, Phys. Lett. **B347**, 394 (1995), hep-ph/9412250.

[34] T. Stelzer and W. F. Long, Comput. Phys. Commun. **81**, 357 (1994), hep-ph/9401258.

[35] D. O. Carlson, Ph.D. Thesis, Michigan State University (1995), hep-ph/9508278.

[36] T. Sjöstrand, Comput. Phys. Commun. **82**, 74 (1994).

[37] G. Marchesini *et al.*, Comput. Phys. Commun. **67**, 465 (1992).

[38] F. A. Berends, R. Kleiss, P. D. Causmaecker, R. Gastmans, and T. T. Wu, Phys. Lett. **B103**, 124 (1981).

[39] R. Kleiss and W. J. Stirling, Nucl. Phys. **B262**, 235 (1985).

[40] Z. Xu, D.-H. Zhang, and L. Chang, Nucl. Phys. **B291**, 392 (1987).

[41] J. F. Gunion and Z. Kunszt, Phys. Lett. **B161**, 333 (1985).

[42] R. Gastmans and T. T. Wu, Oxford, UK: Clarendon (1990) 648 p. (International series of monographs on physics, 80).

[43] M. L. Mangano and S. J. Parke, Phys. Rept. **200**, 301 (1991).

[44] L. Dixon, (1996), hep-ph/9601359.

[45] F. A. Berends, P. H. Daverveldt, and R. Kleiss, Nucl. Phys. **B253**, 441 (1985).

[46] A. Ballestrero and E. Maina, Phys. Lett. **B350**, 225 (1995), hep-ph/9403244.

[47] S. Dittmaier, Phys. Rev. **D59**, 016007 (1999), hep-ph/9805445.

[48] M. Bohm, H. Spiesberger, and W. Hollik, Fortsch. Phys. **34**, 687 (1986).

[49] A. Pukhov *et al.*, (1999), hep-ph/9908288.

[50] H. L. Lai *et al.*, Phys. Rev. **D55**, 1280 (1997), hep-ph/9606399.

[51] A. D. Martin and D. Zeppenfeld, Phys. Lett. **B345**, 558 (1995), hep-ph/9411377.

[52] S. Eidelman and F. Jegerlehner, Z. Phys. **C67**, 585 (1995), hep-ph/9502298.

[53] M. L. Swartz, Phys. Rev. **D53**, 5268 (1996), hep-ph/9509248.

[54] R. Alemany, M. Davier, and A. Hocker, Eur. Phys. J. **C2**, 123 (1998), hep-ph/9703220.

[55] S. Catani, Y. L. Dokshitzer, M. H. Seymour, and B. R. Webber, Nucl. Phys. **B406**, 187 (1993).

[56] A. Denner, S. Dittmaier, M. Roth, and D. Wackeroth, Nucl. Phys. **B560**, 33 (1999), hep-ph/9904472.

[57] G. Mahlon and S. Parke, Phys. Rev. **D53**, 4886 (1996), hep-ph/9512264.

[58] M. Jezabek, Nucl. Phys. Proc. Suppl. **37B**, 197 (1994), hep-ph/9406411.